J. Phys. Chem. A **2000,** *104,* 5495−5502

Infrared Spectra of UO_2, UO_2^+, and UO_2^- in Solid Neon

Mingfei Zhou and Lester Andrews*,†

University of Virginia, Department of Chemistry, Charlottesville, Virginia 22901

Nina Ismail and Colin Marsden*,‡

Laboratoire de Physique Quantique (UMR 5626), IRSAMC, Université Paul Sabatier,
118 Route de Narbonne, F-31062, Toulouse Cedex 4, France

Received: January 24, 2000; In Final Form: April 4, 2000

Reactions of laser-ablated uranium atoms, cations, and electrons with O_2 during condensation with excess neon produce UO, UO_2, UO_3, UO_2^+, and UO_2^- as characterized by infrared spectra with oxygen isotopic substitution and B3LYP/pseudopotential calculations. Differences in low-lying states for UO_2 give rise to substantial shifts and ground state reversal between argon and neon matrices. A series of B3LYP/pseudopotential calculations has been undertaken on oxide species related to the uranyl dication by the addition of one, two, or three electrons. Several electronic states have been characterized for each species. These simple, low-cost calculations predict vibrational frequencies which match those observed in neon matrices extremely well (typically 3−5% too high). The ground state of neutral UO_2 appears to have $^3\Phi_u$ symmetry, while $^2\Phi_u$ ground states are implied for UO_2^+ and UO_2^-.

Introduction

Laser ablation has proven to be an effective means to evaporate the more refractory metals for spectroscopic studies of novel reaction products particularly for the actinide metals uranium[1−6] and thorium.[7,8] With the evolution of this technique, lower laser powers are used, which makes it feasible to employ solid neon to trap small reactive species. Under proper conditions, this matrix isolation method preserves reaction products of ablated atoms, cations, and electrons.[9−15] Neon offers the obvious advantage of being less polarizable, and solid neon often traps a higher yield of cation species than argon. Recent laser-ablation studies in this laboratory with O_4^+, O_6^+, $C_2O_4^+$, $FeCO^+$, and $RhCO^+$ have demonstrated this advantage for the infrared investigation of cations.[9−14]

Uranium provides an important cation, namely, uranyl, UO_2^{2+}, which has been studied in many condensed phase environments, but only in the gas phase[16] can UO_2^{2+} be considered a true dipositive cation as medium polarizability will clearly affect the net electronic charge on the condensed phase species.[17,18] Our first laser-ablation experiments with uranium and oxygen prepared UO_2 based on a strong 776 cm^{-1} band in solid argon,[1] which is in agreement with the original thermal uranium dioxide matrix-isolation experiments.[19] Additional 952.3 and 886.1 cm^{-1} absorptions, attributed to charge-transfer complexes,[19,20] are important because condensed phase uranyl dication absorptions appear in this region.[18]

We have found that the strong antisymmetric stretching fundamental blue shifts 10−20 cm^{-1} upon going from solid argon to solid neon for a number of transition metal dioxides and their anions.[15,21−23] In addition, the actinide oxide ThO blue shifts about 10 cm^{-1}, ThO_2 about 22 cm^{-1}, and UN_2 26 cm^{-1} from solid argon to solid neon.[2,8,24,25] However, cations, which clearly interact more strongly with the matrix medium, often blue shift by larger amounts.[9,11,13] The observation of UO_2 and possible cations in solid neon will increase our understanding of these important species.

In addition to experimental studies, we have performed an extensive series of DFT calculations on UO_2 species with three aims in mind. First, the vibrational frequency calculations will support the experimental assignments and thereby render them more reliable. Second, we wanted to obtain information on the nature of the ground and low-lying electronic states for UO_2 and ions such as UO_2^+ and UO_2^-. Third, a detailed comparison between experimental and computed vibrational frequencies for several related actinide species, some of which are open shell and all of which are subject to important relativistic effects, will provide most useful data and extend the range of chemical systems where DFT methods have been checked and calibrated.

Experimental Methods

The experiment for laser ablation and matrix isolation spectroscopy has been described in detail previously.[1,4,26,27] Briefly, the Nd:YAG laser fundamental (1064 nm, 10 Hz repetition rate with 10 ns pulse width) was focused on the rotating metal uranium target (Oak Ridge National Laboratory) using low energy (1−5mJ/pulse). Laser-ablated metal atoms were co-deposited with oxygen (0.01−0.2%) in excess neon onto a 4K CsI cryogenic window at 2−4 mmol/h for 30 min to 1 h. Oxygen (Matheson) and isotopic $^{18}O_2$ (Yeda) and isotopic mixtures were used in different experiments. Infrared spectra were recorded at 0.5 cm^{-1} resolution on a Nicolet 750 spectrometer with 0.1 cm^{-1} accuracy using a HgCdTe detector. Matrix samples were annealed at different temperatures to allow diffusion and reaction of trapped species, and selected samples were subjected to broadband photolysis by a medium-pressure mercury arc (Philips, 175W, globe removed, $\lambda > 240$ nm) to characterize photosensitive species that might be molecular

---

* To whom correspondence should be addressed.

† E-mail: lsa@virginia.edu.

‡ E-mail: marsden@irsamc1.ups-tlse.fr.

10.1021/jp000292q CCC: $19.00

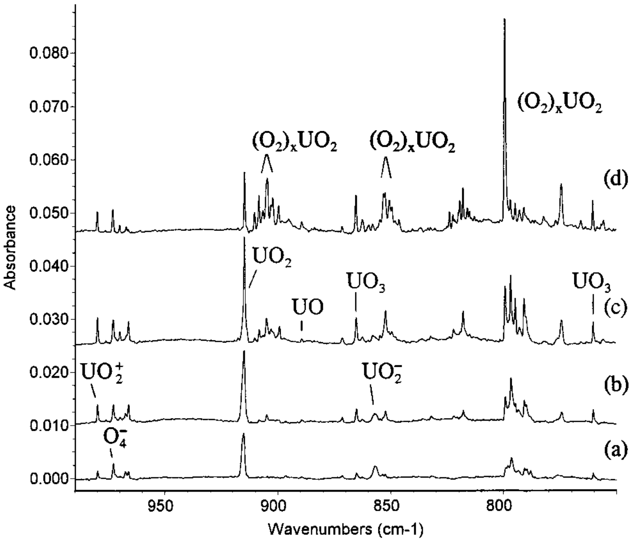

Figure 1. Infrared spectra in the 990−750 cm^{-1} region for laser-ablated uranium with dioxygen in excess neon at 4 K. (a) 0.05% O_2 co-deposited for 30 min, after (b) annealing to 8 K, (c) annealing to 10 K, and (d) annealing to 12 K.

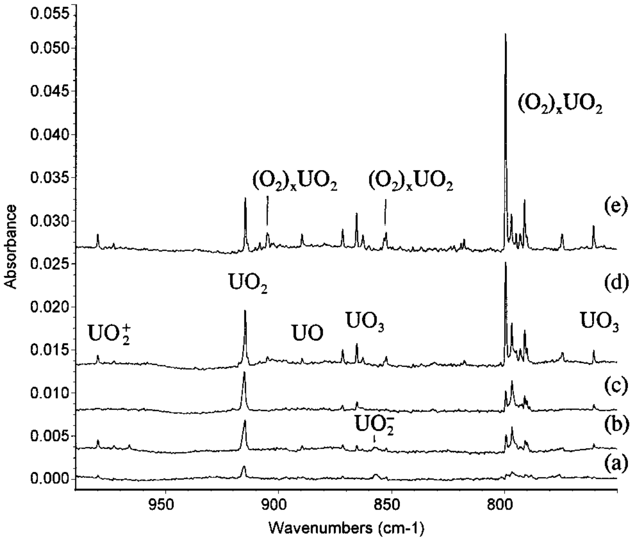

Figure 2. Infrared spectra in the 990−750 cm^{-1} region for laser-ablated uranium with dioxygen in excess neon at 4 K. (a) 0.01% O_2 co-deposited for 30 min, after (b) annealing to 8 K, (c) $\lambda > 240$ nm photolysis, (d) annealing to 10 K, and (e) annealing to 12 K.

anions or cations. Additional experiments were performed with CCl_4 added to the sample at 10% of the O_2 reagent concentration. Previous laser-ablation experiments have shown that added CCl_4 preferentially captures ablated electrons and thereby enhances the yield of molecular cation products and essentially prevents molecular anion products from being formed in the matrix.[9−14]

Experimental Results

Infrared spectra recorded for laser-ablated uranium co-deposited with O_2 diluted in neon onto a 4 K substrate are shown in Figures 1 and 2 with spectra following annealing and photolysis. Product absorptions are listed in Table 1. Bands due to O_4^+ (1164.2 cm^{-1}), O_3 (1039.7, 1038.5 cm^{-1}), and O_4^- (973.0 cm^{-1}) are characteristic of laser-ablated metal oxygen experiments.[11,13,28,29] Investigations were done with $^{18}O_2$, $^{16}O_2$+$^{18}O_2$ mixture, and statistical $^{16}O_2$+$^{16}O^{18}O$+$^{18}O_2$, and spectra from $^{18}O_2$ and $^{16}O_2$+$^{16}O^{18}O$+$^{18}O_2$ samples are illustrated in Figures 3 and 4. The experiment with $^{16}O_2$+$^{18}O_2$ gave the sum of pure isotopic spectra, except for O_4^+, O_4^-, O_3, and UO_3, which produced six absorptions each.

TABLE 1: Infrared Absorptions (cm^{-1}) Observed from Reactions of Laser-Ablated Uranium with Dioxygen in Excess Neon during Condensation at 4 K

$^{16}O_2$	anneal[a]	$^{18}O_2$	new with $^{16}O^{18}O$[b]	16/18 ratio	identification
1164.2	+	1098.8	four	1.0597	O_4^+
1135.2	+	1071.6	too weak	1.0594	$(O_2)_xUO_2$ complex
1039.7	+	982.6	four	1.0581	O_3
1038.5	+	981.4	four	1.0582	O_3 site
1009.3	+	954.1	several	1.0579	O_x^- anion?
980.1	+	931.0	963.5	1.0527	UO_2^+
973.0	−	919.6	four	1.0581	O_4^-
966.2	−	913.2		1.0580	perturbed O_4^-
914.8	+	869.2	900.5	1.0526	UO_2
908.3	+	863.0		1.0525	$(O_2)UO_2$ complex
905.1	+	859.8		1.0527	$(O_2)UO_2$ complex
899.4	+	854.6		1.0524	$(O_2)UO_2$ complex
889.5	+	842.0		1.0564	UO
871.5	+	828.5	> two	1.0519	U_xO_y
865.3	++	822.0	859.7, 854.9, 829.9	1.0527	UO_3
857.2	−	813.9	843.3	1.0532	UO_2^-
852.4	+	809.7		1.0527	$(O_2)_xUO_2$ complex
818.0	+	772.2	?	1.0593	U_xO_y aggregate
799.2	++	759.0	793.7, 748.7	1.0530	$(O_2)_xUO_2$
796.7	+	756.6		1.0530	$(O_2)_xUO_2$
790.8	+	750.5		1.0537	$(O_2)_xUO_2$
774.3	+	736.0		1.0520	?
760.3	++	719.1	746.2, 734.3, 726.5	1.0573	UO_3
616.1	++	583.6	614.8, 600.1, 584.4	1.0557	$((O_2)UO_2^-)$

[a] Annealing behavior: + denotes increase and − indicates decrease. [b] The scrambled isotopic reagent $^{16}O_2$+$^{16}O^{18}O$+$^{18}O_2$ gave the same bands as $^{16}O_2$ and $^{18}O_2$ plus the new bands listed here.

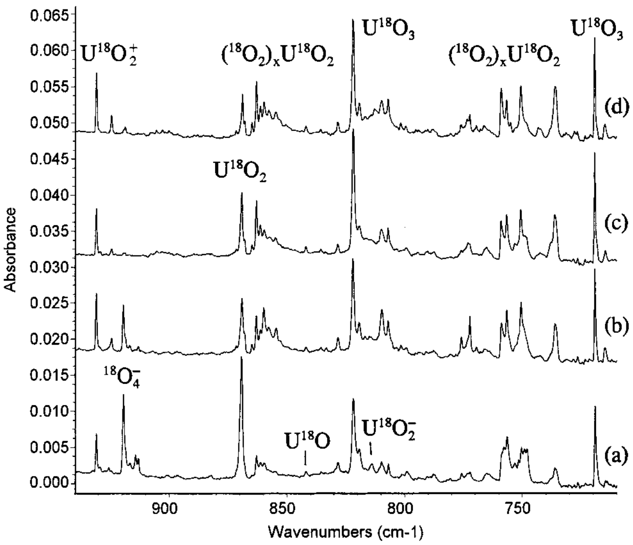

Figure 3. Infrared spectra in the 940−710 cm^{-1} region for laser-ablated uranium with dioxygen in excess neon at 4 K. (a) 0.02% $^{18}O_2$ co-deposited for 30 min, after (b) annealing to 8 K, (c) λ >240 nm photolysis, and (d) annealing to 10 K.

Another experiment conducted with 0.2% O_2 and 0.02% CCl_4 in neon must be compared with the 0.2% O_2 experiment run without CCl_4: product band absorbance ratios on deposition (with CCl_4/without CCl_4) are 1164.2 cm^{-1} (1.2), 1009.3 (0),

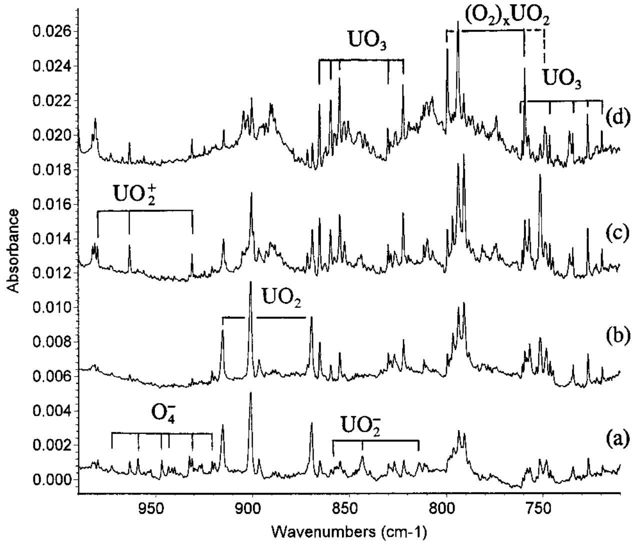

Figure 4. Infrared spectra in the 990−710 cm^{-1} region for laser-ablated uranium with dioxygen in excess neon at 4 K. (a) 0.05% ($^{16}O_2$+$^{16}O^{18}O$+$^{18}O_2$ in 1:2:1 ratio) co-deposited for 30 min, after (b) $\lambda > 240$ nm photolysis, (c) annealing to 10 K, and (d) annealing to 12 K.

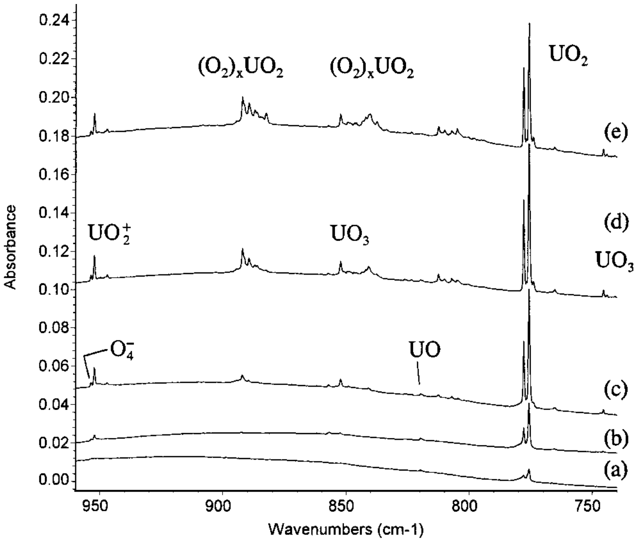

Figure 5. Infrared spectra in the 960−740 cm^{-1} region for laser-ablated uranium with dioxygen in excess argon at 6 K. (a) 0.04% O_2 co-deposited for 30 min, after (b) annealing to 18 K, (c) annealing to 24 K, (d) annealing to 30 K, and (e) annealing to 35 K.

980.1 (2.8), 973.0 (0.05), 914.8 (0.33), 889.5 (1.2), 865.3 (0.5), 857.2 (0), and 616.1 (0.15). Ratios >1 indicate enhancement with CCl_4 added, and ratios <1 show reduction with CCl_4 present.

Argon matrix uranium experiments (0.4 and 0.04% O_2) were performed on a 6 K substrate, and spectra for the more dilute sample are shown in Figure 5 including sample annealing. Absorptions are, of course, weaker than those in the previous higher laser power, higher O_2 concentration 12 K experiments, but band positions are the same.[1] Note the dramatic increase of sharp bands at 777.9 and 775.7 cm^{-1} upon annealing, but the major difference in argon is the absence of a nearby counterpart for the 914.8 cm^{-1} neon matrix band.

Two investigations employed a UO_2 ceramic target for laser ablation. The first experiment co-deposited ablated material with neon, and the spectrum is shown in Figure 6; the major absorptions are the same as with U and O_2, but populations are different. Most notable are the absence of O_4^+ and O_4^-, and very weak O_3, which require excess O_2, and an increase in the 889.5 and 871.5 cm^{-1} bands. The second study co-deposited ablated material with 0.05% $^{18}O_2$ in neon, and the isotopic band populations are again different; this experiment provides mechanistic information, which will be described later.

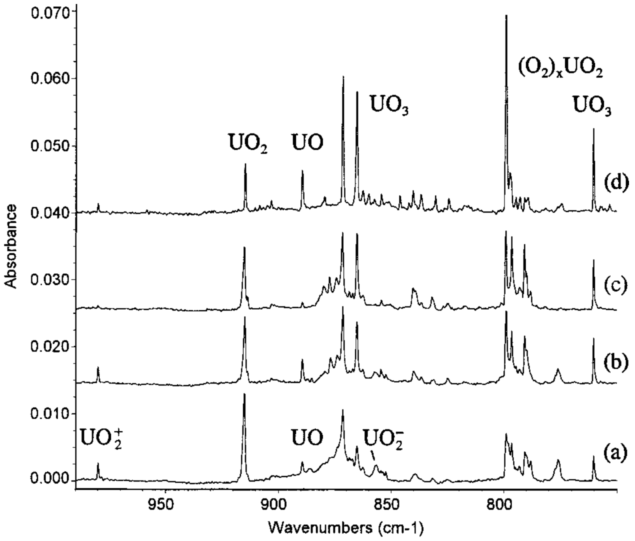

Figure 6. Infrared spectra in the 990−750 cm^{-1} region for laser-ablated uranium oxide material trapped in excess neon at 4 K. (a) sample co-deposited for 30 min, after (b) annealing to 8 K, (c) $\lambda > 240$ nm photolysis, and (d) annealing to 12 K.

Complementary uranium experiments also performed with N_2O (0.2%) in neon. The major product absorption is at 889.5 cm^{-1} with sharp weaker bands at 1076.6, 1072.6, 980.1, 914.8, and 865.4 cm^{-1}. In contrast to the O_2 experiments, annealing produced only a very weak sharp 799.1 cm^{-1} band.

Theoretical Methods

Calculations were performed on several uranium oxygen species and on UN_2 using the Gaussian 98 program.[30] While test calculations were undertaken at the SCF level, these will not be described here as it is well-known that they do not give quantitatively satisfactory results for vibrational frequencies. In the case of the uranyl dication (UO_2^{2+}), we have shown recently that density functional theory (DFT) performs particularly well, giving vibrational wavenumbers that are comparable to CCSD or CCSD(T) values obtained with fully relativistic (four-component) methods.[31] We favor the hybrid variant of DFT known as B3LYP.[32,33] We have also shown that pseudopotential methods are quite suitable for the uranyl ion, provided that a "small core" is adopted for uranium. In this work we employed the pseudopotential developed in Stuttgart, which leaves 32 electrons to be described explicitly: the 5s, 5p, 6s, 6p, 6d, 5f, and 7s orbitals of the U atom. Our basis for uranium was essentially that proposed by the Stuttgart group,[34] flexibly contracted for a U^{4+} ion, supplemented with an additional diffuse f-type function (exponent 0.08). For oxygen and nitrogen, we adopted pseudopotentials and bases developed in Toulouse;[35] the bases are of "double-ζ plus polarization plus diffuse" quality. The "ultrafine" grid was adopted for numerical integration.

In an attempt to evaluate the consequences for vibrational frequency calculations of the lack of g-type functions in the uranium basis, tests were performed on the uranyl dication. At the B3LYP level of theory, an exponent of 0.75 is roughly optimum in the variational sense. As a set of such functions was found to lead to changes judged to be insignificant (a reduction in the U═O bond length of just 0.004 Å, an energy

TABLE 2: Calculated States, Relative Energies, Structures and Vibrational Frequencies for Uranium Oxide Species and UN_2

molecule	state	relative energy[a]	bond length, Å	angle, deg	frequencies, cm^{-1}
UO	$^5\Gamma$		1.850		846
UO_2^{2+}	$^1\Sigma_g^+$		1.705	180	1041 (σ_g), 161 (π_u), 1140 (σ_u)
UO_2^+	$^2\Phi_u$	0	1.764	180	936 (σ_g), 148 (π_u), 1010 (σ_u)
	$^2\Delta_u$	21	1.751	180	948 (σ_g), 172 (π_u), 1017 (σ_u)
UO_2	$^3\Phi_u$	0	1.800	180	874 (σ_g), 138 (π_u), 931 (σ_u)
	$^3\Delta_u$	17	1.787	180	883 (σ_g), 161 (π_u), 936 (σ_u)
	^3H_g	23	1.853	180	792 (σ_g), 35 (π_u), 814 (σ_u)
UO_2^-	$^2\Phi_u$	0	1.828	180	825 (σ_g), 136 (π_u), 874 (σ_u)
	$^2\Delta_u$	13	1.817	180	830 (σ_g), 156 (π_u), 876 (σ_u)
	^4H_g	37	1.901	180	723 (σ_g), 38i (π_u), 735 (σ_u)
UO_3 (C_{2v})	$^1A_1$		1.810	100.6	887 (a_1, 34), 885 (b_2, 479), 782 (a_1, 209)[b]
			1.853	158.8	
$(UO_2^+)(O_2^-)$	$^1A_1$	0	1.794	160.6	936 (a_1, 41), 925 (b_2, 435), 854 (a_1, 93), 529 (a_1, 59)[b]
			2.108	40.0	
			1.443		
	$^3B_2$	47	1.807	169.6	1200 (a_1, 20), 907 (b_2, 428), 855 (a_1, 11) 379 (a_1, 81)[b]
			2.371	32.8	
			1.339		
UN_2	$^1\Sigma_g^+$		1.731	180	1071 (σ_g), 102 (π_u), 1118 (σ_u)

[a] Units in kJ/mol. [b] Intensities, in km/mol, are given for selected bond stretching modes, after the symmetry.

lowering of only 7 mH and an increase in the antisymmetric stretching frequency of less than 2 cm^{-1}), they were not included in the remaining calculations. We also checked that the influence of adding h-type functions to the U basis was, as might be expected, even smaller than that found for g-types; a reduction in bond length of the order of 0.001 Å, an energy lowering of 0.7 mH and an decrease in the antisymmetric stretching frequency of just 0.2 cm^{-1}.

Several tests were performed to ensure that the basis used was sufficiently extensive for the molecules in question. The total energy of the ground state of the neutral UO_2 was found to change by less than 0.2 kJ/mol when extra, more diffuse, functions of each type (s, p, d ,and f) were added to the basis, while the energy difference between the ground and first excited state changed by far less than that. These differences were judged to be insignificant.

Calculations on open-shell systems were performed using spin-unrestricted methods, as these allow the calculation of vibrational frequencies to be more efficient. Spin contamination was not serious, as the value of $\langle S^2 \rangle$ never exceeded 0.76 for a doublet, 2.02 for a triplet, or 3.77 for a quartet state. Spin−orbit effects have not been treated explicitly in this work. As a result, the relative energies of different electronic states for a given species may be in error by a small amount. In the case of PuO_2^{2+}, which is isoelectronic with UO_2, the relative energies of a series of states, calculated with and without explicit consideration of spin−orbit coupling, differ by about 8 kJ/mol.[36] However, because spin−orbit effects are primarily atomic in nature, we believe that they will have little influence either on bond lengths or on vibrational frequencies. While it is not possible at present to justify this expectation rigorously, the excellent agreement with the experimental neon matrix data reported here provides empirical support.

Theoretical Results

Results of the B3LYP calculations are summarized in Table 2, where the principal optimized geometrical parameters and the harmonic vibrational frequencies (for ^{238}U and ^{16}O or ^{14}N) are presented. The results for UO_2^{2+} are slightly different from those reported previously;[31] because the earlier values were obtained by double numerical differentiation of energies, whereas the current data are obtained directly from analytical second derivatives of the energy, it is clear that the present results are more reliable. Individual species are considered in the order UO_3, UN_2, UO_2^+, UO_2, UO_2^-, and "UO_4", which is better written as a complex between UO_2^+ and O_2^-.

UO_3 has already been studied at the SCF level by Pyykkö and co-workers,[37] who described a planar, almost T-shaped species with C_{2v} symmetry. At the B3LYP level of theory the main structural features are retained, but the difference between the two shorter (1.81 Å) and one longer (1.85 Å) U−O bond is diminished. The most intense stretching modes are predicted at about 891 (b_1) and 779 (a_1) cm^{-1}, substantially lower values than the previous SCF results. The D_{3h} geometry for UO_3 is not a true minimum; it has a doubly degenerate imaginary in-plane bending frequency that leads to the T-shaped minimum, 16 kJ/mol lower in energy.

UN_2 is a particularly interesting molecule as it is isoelectronic with the uranyl dication. Since UN_2 is neutral, its interaction with a rare gas matrix will be much weaker than that with UO_2^{2+}, and the calculated vibrational frequencies therefore serve as a valuable calibration. Our B3LYP value for the IR-active σ_u stretching mode of UN_2 is 1118 cm^{-1}, slightly lower than the corresponding uranyl result of 1140 cm^{-1}, and slightly higher than the 1076.6 cm^{-1} value observed for UN_2 in solid neon.[25]

The electronic structures of the various possible states of UO_2^+, UO_2, and UO_2^- are most naturally considered by reference to the (closed-shell) uranyl dication. We find the lowest-lying virtual orbitals for uranyl, in order of increasing energy, to be ϕ_u, δ_u, π_u, δ_g, σ_g, and σ_u. Although the calculated energies of virtual orbitals must be treated with prudence, the lowest lying virtuals offer valuable guidance as to states that need to be considered for species containing extra electrons. (It should be noted that the energy ordering of the virtual orbitals is not the same at the SCF and B3LYP levels of theory).

The first two virtuals of ϕ_u and δ_u symmetries are rigorously nonbonding between uranium and oxygen, as they are purely f-type atomic orbitals on uranium. We have characterized $^2\Phi_u$, $^2\Delta_u$, $^2\Pi_u$, $^2\Sigma_g$, and $^2\Delta_g$ states of UO_2^+ by computation. These are listed in order of increasing relative energy, showing that aufbau arguments are useful but not infallible. While the $^2\Phi_u$ and $^2\Delta_u$ states are close in energy, only 21 kJ/mol, the others are at least 150 kJ/mol above the ground state and their details will be presented elsewhere.

The bond length in the $^2\Phi_u$ ground state of UO_2^+ is almost 0.06 Å longer and the σ_u frequency 130 cm^{-1} lower than those in the uranyl dication, despite the nonbonding nature of the ϕ_u orbital occupied by the unpaired electron. While Mulliken charges should not be taken too literally, the trends observed for related species are informative. At the B3LYP level, we find a net charge of +2.44 e on U in uranyl, but +1.97 *e* in UO_2^+. Natural charges on U in uranyl and UO_2^+ are +3.30 and +2.79 *e*, respectively; the difference between these values is almost exactly the same as the difference between the two Mulliken charges. These results remind us that there can be considerable coupling between charge flows in different symmetries, so that even if the "additional" electron in UO_2^+ is formally localized on U, the net charges suggest that it is almost 50% delocalized onto the oxygen atoms. However, the spin density on U is in fact slightly greater than unity (1.09), consistent with the localization interpretation.

Since the ϕ_u and δ_u virtual orbitals in uranyl are so close in energy, the most plausible configuration for the ground state of neutral UO_2 involves single occupation of each orbital to give ^3H_g symmetry.[38,39] This occupation pattern has been reported for the plutonyl dication,[31] which is isoelectronic with neutral UO_2. To our considerable surprise, we found that the configurations with one unpaired electron in the σ_g orbital and one in either the ϕ_u or δ_u manifolds, yielding $^3\Phi_u$ or $^3\Delta_u$ states, respectively, are both slightly more stable than the ^3H_g state; note that this σ_g orbital is the LUMO+4 in uranyl. Using the B3LYP method, the ground state is found to be $^3\Phi_u$, but the $^3\Delta_u$ and ^3H_g states are only 17 and 23 kJ/mol higher, respectively. As for the two doublet states of UO_2^+, these two ungerade states have very similar bond lengths and stretching frequencies, and so cannot be distinguished by the present matrix IR data. However, the σ_u frequency for the ^3H_g state is over 100 cm^{-1} lower. Using instead the 6-31+G* basis set for O gives essentially the same frequencies.

The optimized bond distance for the UO_2 ground state is nearly 0.04 Å longer than that in the monocation, or 0.10 Å longer than in uranyl dication. This further increase in bond length leads to a 79 cm^{-1} decrease in the σ_u frequency. The Mulliken net charge on U in UO_2 is +1.26 *e* and the spin density is 2.07. It is interesting to note that the energy separation between the $^3\Phi_u$ and $^3\Delta_u$ states of UO_2 (17 kJ/mol) is similar to that between the $^2\Phi_u$ and $^2\Delta_u$ states of UO_2^+ (21 kJ/mol). An AQCC calculation based on orbitals obtained using CAS methods also predicts that the ground state of UO_2 has $^3\Phi_u$ symmetry, and the ^3H_g state is 35 kJ/mol higher.[40]

Our computed first and second ionization energies of UO_2 are 605 and 1476 kJ/mol, or 6.27 and 15.31 eV. These values do not include any zero-point effects, which are insignificant (only a few kJ/mol). They compare relatively well with the experimental results of 5.4 (0.1) and 15.4 (2.6) eV, respectively,[16,39] providing a further indication of the success of the B3LYP method for these systems.

The three lowest states of the UO_2^- anion, by B3LYP computation, possess $^2\Phi_u$, $^2\Delta_u$ and ^4H_g symmetries (in order of increasing energy). The low-lying doublet states involve double occupation of the σ_g orbital already mentioned for neutral UO_2, while in the quartet state the ϕ_u, δ_u, and σ_g orbitals are all singly occupied. Following the pattern already established for UO_2^+ and UO_2, occupation of the ϕ_u orbital in the anion is more favorable than for the δ_u, by a small margin of only 13 kJ/mol; once again, the properties of the $^2\Phi_u$ and $^2\Delta_u$ states do not allow us to distinguish between them. The ^4H_g state is not a true minimum. The increase in bond length and decrease in stretching frequency of only 0.03 Å or 57 cm^{-1} for the anion are relatively small, consistent with an appreciable electron affinity of 108 kJ/mol (1.1 eV). We are not aware of any experimental value for this quantity.

Two different "complexes" of UO_2^+ and O_2^- with C_{2v} symmetry have been characterized. Analysis of the computed wave functions shows that this description is more realistic than either UO_4 or $(UO_2^{2+})(O_2^{2-})$. Because UO_2^+ and O_2^- are both doublets, singlet and triplet states are possible for these complexes; the singlet is found to be substantially more stable (47 kJ/mol) than the triplet. The geometries of the two species are similar, but the O−O distance in the triplet (1.339 Å) is significantly less than in the singlet (1.443 Å). In isolated O_2^- the predicted O−O distance (1.359 Å) is intermediate between these two values.

Discussion

The uranium oxides in solid neon will be identified by oxygen isotopic substitution, by comparison with argon matrix work, and by density functional calculations.

UO_3. The stable uranium trioxide species in solid neon will be identified first by straightforward comparison to the argon matrix work. Gablenick et al. conclusively identified T-shaped UO_3 from two strong infrared bands at 852.6 and 745.6 cm^{-1} and additional mixed oxygen isotopic spectra.[41] Our laser-ablated U atom reactions with O_2 in argon[1] gave sharp bands at 852.5 and 745.5 cm^{-1} with 16/18 isotopic ratios 1.0525 and 1.0572, which are in excellent agreement. The present neon matrix experiments produced sharp 865.3 and 760.3 cm^{-1} bands with 16/18 isotopic ratios 1.0527 and 1.0573, which increased 6 times upon annealing. The small (12.8 and 14.8 cm^{-1}) blue shifts from argon-to-neon, the virtually unchanged isotopic frequency ratios, and similar mixed isotopic spectra clearly identify the same UO_3 molecule in solid neon. Upon annealing, UO_3 is made by the reaction of UO and O_2 as will be discussed below for UO ablated from UO_2 ceramic reacting with $^{18}O_2$.

The vibrational frequencies predicted for the most intense stretching modes at the B3LYP level, 891 (b_1) and 779 cm^{-1} (a_1), are 3.0 and 2.5% higher than the observed neon matrix values. Clearly, the present B3LYP calculations provide a useful approximation for observed uranium oxide vibrational frequencies.

UO_2. The neon matrix spectra for 0.05 and 0.01% O_2 (Figures 1 and 2) show that the 914.8 cm^{-1} band is dominant on deposition under low concentration conditions, and that this band increases slightly on annealing to allow diffusion and further reaction of O_2. It thus appears that the 914.8 cm^{-1} band is due to the primary U+O_2 reaction product.

The 914.8 cm^{-1} band exhibits a 1/2/1 relative intensity triplet pattern at 914.8, 900.5, 869.2 cm^{-1} with $^{16}O_2$+$^{16}O^{18}O$+$^{18}O_2$ (Figure 4) for the vibration of two equivalent oxygen atoms, and the 16/18 isotopic ratio 1.0526 is just below the harmonic value (1.0530) calculated for the σ_u mode of linear OUO. This band is assigned to the σ_u mode of ground state $^3\Phi_u$ UO_2 in solid neon. The 914.8 cm^{-1} neon matrix observation is in excellent agreement with our B3LYP value of 931 cm^{-1}. The formation of UO_2 is spontaneous on deposition and on annealing to 10 K. Therefore, reaction 1, which is calculated (B3LYP) to be highly exothermic, is believed to proceed by direct insertion with little or no activation energy. In the $^{16}O_2$+$^{18}O_2$ experiment, only the 914.8 and 869.2 cm^{-1} bands are observed and they increase 25% on annealing to 8 K with *no* $^{16}OU^{18}O$ absorption at 900.5 cm^{-1} before or after annealing. This evidence shows that UO_2 is made by reaction with a *single* O_2 molecule, and the concerted reaction, most likely insertion, is the direct way to make a linear molecule with two equivalent oxygen atoms.

Spontaneous growth of TiO_2, ZrO_2, and HfO_2 has also been observed in solid argon[42] upon annealing at 25 K, and these insertion reactions are not as exothermic as reaction 1.

$$U + O_2 \rightarrow OUO \qquad (\Delta E = -980 \text{ kJ/mol}) \qquad (1)$$

How then can we account for the original[1,19] identification of UO_2 in solid argon at 775.7 cm^{-1}? The vibrational red shift from 914.8 to 775.7 cm^{-1} is too much for a simple matrix interaction. Note that the σ_u frequency calculated for the ^3H_g state at 814 cm^{-1} is in reasonable agreement with the argon matrix value for UO_2. We believe that the ^3H_g state interacts sufficiently strongly with the argon matrix to become the ground state in solid argon. Precedent exists for reversal of ground states in different matrix media: see Ag_3, for example.[43,44] There is, of cource, some neon matrix shift from the gas phase value, but this is expected to be relatively small on the order of 10−20 cm^{-1}.

Argon is substantially more polarizable than neon (more than 4 times). The calculated charge distribution in the upper ^3H_g state is appreciably more ionic than in the ground $^3\Phi_u$ state: as an indication, the Mulliken net charges on U are +1.49 and +1.26 e in the ^3H_g and $^3\Phi_u$ states, respectively. We therefore suggest that the more polar character of the excited state leads to sufficient extra polarization of the argon matrix to make it the favored lower energy species in that environment. Unfortunately this argument, while plausible, cannot be made quantitative at present.

$(O_2)_xUO_2$ Complexes. The 905.1, 852.4, and 799.2 cm^{-1} bands increase more dramatically than the 914.8 cm^{-1} band upon annealing in solid neon. The 799.2 cm^{-1} absorption also exhibits a triplet absorption for the vibration of two equivalent oxygen atoms and these bands exhibit 16/18 ratios appropriate for σ_u vibrations of linear OUO subunits. The 905.1, 852.4, and 799.2 cm^{-1} bands are due to $(O_2)_xUO_2$ complexes involving ground state $(^3\Phi_u)UO_2$. The first such complex ($x = 1$) has a calculated b_2 UO_2 frequency of 925 cm^{-1}, a small red shift from isolated UO_2, and the 905.1 cm^{-1} neon matrix band is assigned accordingly. The present B3LYP calculations suggest that $(O_2)UO_2$ can be represented as $(UO_2^+)(O_2^-)$ as the Mulliken charge on U is + 2.01, nearly the same as that in UO_2^+ and the dipole moment is large (5.2 D). Similar polar character has been found for $(O_2)IrO_2$.[45] The reaction of O_2 and UO_2, eq 2, is exothermic by 297 kJ/mol at the B3LYP level. The 852.4 and 799.2 cm^{-1} bands are assigned to higher $(O_2)_xUO_2$ complexes with UO_2 in the $^3\Phi_u$ ground state in solid neon. The large $914.8 - 799.2 = 115.6$ cm^{-1} red shift for large x value is comparable to that observed for UN_2 (1076.6 cm^{-1}) with sequential addition of N_2 ligands forming a series of bands terminating at 1000.0 cm^{-1} due to fully ligated $(N_2)_xUN_2$ in solid neon.[8,25]

$$O_2 + UO_2 \rightarrow (O_2)UO_2 \qquad (\Delta E = -297 \text{ kJ/mol}) \quad (2)$$

The 616.1 cm^{-1} band was favored with higher O_2 concentration and increased slightly on annealing and photolysis. This band revealed a sextet at 616.1, 613.5, 601.2, 599.2, 585.3, and 583.6 cm^{-1} with $^{16}O_2 + {}^{18}O_2$ and a nonet with the statistical isotopic sample (Table 1). Doping with CCl_4 reduced the band to 15% of its yield without CCl_4. Preliminary calculations show that the $^2A_1$ anion $(O_2)UO_2^-$ is 186 kJ/mol below the neutral species and has a strong OUO mode computed at 741 cm^{-1}. The 616.1 cm^{-1} band is tentatively assigned to a $(O_2)UO_2^-$ species.

UO. The weak 889.5 cm^{-1} band increases slightly on annealing and exhibits the 1.0564 isotopic 16/18 ratio, which is slightly lower than the harmonic UO value (1.0566); this is the only diatomic isotopic frequency ratio found here. The increase in 889.5 cm^{-1} band yield with UO_2 ablation and in the U+N_2O reaction further support the UO assignment. This neon matrix band, is, however, *blue shifted* 69.7 cm^{-1} from the argon matrix UO band at 819.8 cm^{-1}. Here UO comes from decomposition of OUO made by reaction of the more energetic ablated U atoms.

Kaledin and Heaven have analyzed nine low-lying electronic states of UO that correlate with either $U^{2+}(5f\ ^37s)\ O^{2-}$ or $U^{2+}(5f\ ^27s^2)\ O^{2-}$ configurations, which have deperturbed harmonic vibrational frequencies near 846 and 935 cm^{-1}, respectively.[46] It appears that the argon and neon matrix interactions also affect the mixing of configurations, and the ground state in a particular environment may change, as UO absorbs at 819.8 cm^{-1} in solid argon and at 889.5 cm^{-1} in solid neon, analogous to the OUO molecule. This is, however, not the case for the thorium oxide molecule, ThO, where argon matrix, neon matrix, and gas-phase fundamentals are 878.8, 887.1, and 891.0 cm^{-1}, respectively.[8,24,47]

UO_2^+. The sharp 980.1 cm^{-1} band increases slightly upon annealing and disappears on photolysis. The 980.1 cm^{-1} band gives a 1/2/1 triplet at 980.1, 963.5, 931.0 cm^{-1} with $^{16,18}O_2$ (Figure 4) for the vibration of two equivalent O atoms, and the 16/18 ratio, 1.0527, again indicates a linear OUO species. The observation of a 1/1 doublet at 980.1, 931.0 cm^{-1} with $^{16}O_2 + {}^{18}O_2$ shows that a single O_2 molecule is involved. Changes in O_2 concentration demonstrate that the sharp 980.1 cm^{-1} band is not O_2 concentration dependent and that it, too, is a primary reaction product. The 980.1 cm^{-1} band is blue shifted 27.8 cm^{-1} from the 952.3 cm^{-1} argon matrix counterpart, which is blue shifted 12.1 cm^{-1} from the krypton matrix counterpart.[1] Although this region is representative of condensed phase uranyl σ_u vibrations,[18] solute and/or anion interactions with the UO_2^{2+} dication must be ignored in order to consider these absorptions characteristic of isolated UO_2^{2+}.

Our B3LYP calculation predicts the isolated UO_2^{2+} σ_u fundamental at 1140 cm^{-1}, which is about 200 cm^{-1} higher than the condensed phase measurements ascribed to UO_2^{2+}. We believe that the condensed phase measurements[18] are made on a UO_2^{2+} moiety which has in fact been partially neutralized by solvent and/or anion polarization. Furthermore, the second ionization energy (IE) of UO_2 (15.4 ± 2.6 eV) is in the range of the first IE of argon (15.8 eV) and extensive polarization is expected for UO_2^{2+} in argon such that the dication cannot be isolated in solid argon. However, the first IE of UO_2 (5.4 eV) is in the range for cations that can be isolated in solid argon.[9,39] The same DFT calculation finds a $^2\Phi_u$ ground-state UO_2^+ with σ_u mode at 1010 cm^{-1}, which is 3.1% higher than the 980.1 cm^{-1} neon matrix observation. Note that B3LYP σ_u frequencies for UO_2^{2+}, UO_2^+ and UO_2 ground states decrease from 1140 to 1010 to 931 cm^{-1} (Table 2).

The dramatic increase (2.8 times) in the 980.1 cm^{-1} band with CCl_4 added strongly supports the cation identification as CCl_4 captures electrons from the ablation process and thus allows the survival of more cations without significant interference to the U+O_2 reaction.[9−14] The 980.1 cm^{-1} band is here assigned to isolated UO_2^+ in solid neon, and the argon matrix 952.3 cm^{-1} band is reassigned to UO_2^+ in solid argon. In addition to U atoms, U^+ is produced by laser ablation,[48] and the UO_2^+ cation is formed here by insertion reactions of U^+ with O_2 during sample deposition and upon annealing, reaction 3, which is also calculated (B3LYP) to be highly exothermic.

$$U^+ + O_2 \rightarrow OUO^+ \qquad (\Delta E = -927\ \text{kJ/mol}) \qquad (3)$$

We have just prepared the NUO^+ cation characterized in the gas phase[48] by reaction of U^+ with NO in solid neon and offer the observed frequencies (1118.6, 969.8 cm^{-1})[25] as a model for the isoelectronic isolated UO_2^{2+} cation. These frequencies are much higher than condensed phase uranyl frequencies,[18] owing to perturbations by the medium. We note that B3LYP pseudopotential stretching frequencies calculated for isolated UO_2^{2+} (1140, 1041 cm^{-1}) and NUO^+ (1191, 1005 cm^{-1})[25] have nearly the same average.

UO_2^-. A weak 857.2 cm^{-1} band is decreased upon annealing at 8 and 10 K and destroyed by ultraviolet photolysis. This band shows a 1/2/1 triplet for two equivalent O atoms and a 16/18 ratio (1.0532) near that for a linear OUO unit. The 857.2 cm^{-1} band is not present with CCl_4 added to the sample as the chlorocarbon preferentially captures most of the ablated electrons and prevents molecular anion formation;[9−14] note that the strong O_4^- band is almost eliminated as well. The 857.2 cm^{-1} absorption is assigned to UO_2^- made by the electron-capture reaction 4, which is calculated to be exothermic. Our DFT calculations find a $^2\Phi_u$ ground state for UO_2^- with a σ_u frequency at 874 cm^{-1}, which is in excellent agreement with the neon matrix observation.

$$OUO + e^- \rightarrow OUO^- \qquad (\Delta E = -108\ \text{kJ/mol}) \qquad (4)$$

Solid UO_2 Ablation. Laser ablation of solid UO_2 gave similar neon matrix spectra to the U+O_2 reaction (compare Figures 1 and 6). The major difference is a 4× enhancement of UO (889.5 cm^{-1}) and 15× increase in the 871.5 cm^{-1} band with the solid. Accordingly, the latter band is presumed due to a higher oxide. Mass spectrometric studies of material ablated from solid uranium dioxide reveal UO_2, UO and UO_3 molecules,[49] and electronic spectroscopy has characterized UO ablated from the oxidized uranium metal surface.[46] We conclude that some of the UO absorption in Figure 6 arises from ablated UO and the rest from atomic recombination.

The solid UO_2 ablation into 0.05% $^{18}O_2$ in neon gave interesting mechanistic results. The composite $U^{18}O_3$ and 18-U(-16)-18 band (822.1 cm^{-1}) and 18-U(-18)-16 (854.9 cm^{-1}) band were 2 times the intensity of the $U^{16}O_3$ band (865.3 cm^{-1}), and the 18-U(-16)-16 (859.6 and 829.9 cm^{-1}) bands were weaker (by factors of 0.8 and 0.2, respectively). Furthermore, the 18-U(-18)-16 band (726.5 cm^{-1}) was far stronger than that of the 18-U(-16)-18 band (734.3 cm^{-1}). This suggests that UO_3 is formed by UO reaction with O_2 through insertion, but the intermediate relaxes *asymmetrically* (C_s product) in preference to *symmetrically* (to give the C_{2v} isomer). The symmetrical transition state is suggested by observation of the C_{2v} isotopic isomer. The yields of $U^{18}O_2^+$, $U^{18}O_2$ and $(O_2)_xU^{18}O_2$ exceed (by 1.5−2 times) the yields of the $^{16}O_2$ species and $^{16}O^{18}O$ counterparts are very weak. This suggests that some $U^{16}O$ and $U^{16}O_2$ are ablated, but that even more atomic U is ablated for reaction with $^{18}O_2$, and that the concentration of ablated species is less than the $^{18}O_2$ concentration (0.05%). Finally, $U^{16}O$ (889.5 cm^{-1}) band is >5 times stronger than that of $U^{18}O$ (842.0 cm^{-1}). This again shows that UO is ablated from the solid and the U reaction with $^{18}O_2$ forms mostly $U^{18}O_2$ with little decomposition to $U^{18}O$.

Conclusions

Reactions of laser-ablated uranium atoms, cations and electrons with O_2 during condensation with excess neon produce UO, UO_2, UO_3, UO_2^+ and UO_2^- as characterized by infrared spectra with oxygen isotopic substitution and B3LYP/pseudopotential calculations. Differences in low-lying $^3\Phi_u$ and ^3H_g states give rise to substantial shifts and ground-state reversal between argon and neon matrices for UO_2. The UO_2^+ absorption at 980.1 cm^{-1} in solid neon is in a region ascribed from condensed phase spectra to uranyl dication, but anion/solvent polarizations partially neutralize the uranyl dication species in condensed phases and reduce the σ_u frequency from the value expected for the isolated uranyl dication.

Simple, low-cost B3LYP calculations have been shown to be astonishingly reliable for the prediction of neon matrix vibrational frequencies, for both open- and closed-shell systems, and for neutrals, positively and negatively charged species, despite the neglect of explicit spin−orbit effects. We have nine different comparisons of observed and computed wavenumbers; the mean error in the computed value is 2.6% while the range is from 0.9 to 5.1%. As we have a substantial number of cases whose chemical nature differs yet achieve a high level of consistency (far higher than we were initially expecting), we can eliminate any possibility of coincidence. Aufbau-based arguments that use energies for virtual orbitals obtained from B3LYP calculations are shown to be unreliable for species related to the uranyl dication. The ground state of neutral UO_2 appears to have $^3\Phi_u$ symmetry, rather than ^3H_g as supposed to date. Systematic trends are uncovered in the bond lengths and vibrational frequencies for the series UO_2^{2+}, UO_2^+, UO_2 and UO_2^-.

Acknowledgment. We gratefully acknowledge N.S.F. support for this research under Grant CHE 97-00116 and IDRIS for computer time (Project 991104).

References and Notes

(1) Hunt, R. D.; Andrews, L *J. Chem. Phys.* **1993**, *98*, 3690.

(2) Hunt, R. D.; Yustein, J. T.; Andrews, L. *J. Chem. Phys.* **1993**, *98*, 6070.

(3) Hunt, R. D.; Thompson, C. A.; Hassanzadeh, P.; Andrews, L. *Inorg. Chem.* **1994**, *33*, 388. Souter P. F.; Andrews, L. *J. Mol. Struct.* **1997**, *412*, 161.

(4) Kushto, G. P.; Souter, P. F.; Andrews, L.; Neurock, M. *J. Chem. Phys.* **1997**, *106*, 5894.

(5) Souter, P. F.; Kushto, G. P.; Andrews, L.; Neurock, M. *J. Am. Chem. Soc.* **1997**, *119*, 1682.

(6) Zhou, M. F.; Andrews, L.; Li, J.; Bursten, B. E. *J. Am. Chem. Soc.* **1999**, *121*, 9712.

(7) Souter, P. F.; Kushto, G. P.; Andrews, L.; Neurock, M. *J. Phys. Chem. A* **1997**, *101*, 1287.

(8) Kushto, G. P.; Souter, P. F.; Andrews, L. *J. Chem. Phys.* **1998**, *108*, 7121. Kushto, G. P.; Andrews, L. *J. Phys. Chem. A* **1999**, *103*, 4836. Zhou, M. F.; Andrews, L. *J. Chem. Phys.* **1999**, *111*, 11044.

(9) Zhou, M. F.; Chertihin, G. V.; Andrews, L. *J. Chem. Phys.* **1998**, *109*, 10893.

(10) Zhou, M. F.; Andrews, L. *J. Am. Chem. Soc.* **1998**, *120*, 11499.

(11) Zhou, M. F.; Hacaloglu, J.; Andrews, L. *J. Chem. Phys.* **1999**, *110*, 9450.

(12) Zhou, M. F.; Andrews, L. *J. Chem. Phys.* **1999**, *110*, 6820.

(13) Zhou, M. F.; Andrews, L. *J. Chem. Phys.* **1999**, *110*, 10370.

(14) Zhou, M. F.; Andrews, L. *J. Phys. Chem. A.* **1999**, *103*, 7773.

(15) Zhou, M. F.; Andrews, L. *J. Chem. Phys.* **1999**, *111*, 4230.

(16) Cornehl, H. H.; Heinemann, C.; Marcado, J.; Pires de Matos, A.; Schwarz, H. *Angew. Chem., Int. Ed. Engl.* **1996**, *35*, 891.

(17) Ohwada, K. *Spectrochim. Acta A* **1975**, *31*, 973.

(18) Gal, M.; Groggin, P. L.; Mink, J. *Spectrochim. Acta A* **1992**, *48*, 121.

(19) Gabelnick, S. D.; Reedy, G. T.; Chasanov, M. G. *J. Chem. Phys.* **1973**, *58*, 4468.

(20) Green, D. W.; Gabelnick, S. D.; Reedy, G. T. *J. Chem. Phys.* **1976**, *64*, 1697.

(21) Chertihin, G. V.; Bare, B. W.; Andrews, L. *J. Phys. Chem. A* **1997**, *101*, 5090.

(22) Chertihin, G. V.; Bare, W. D.; Andrews, L. *J. Chem. Phys.* **1997**, *107*, 2798.

(23) Zhou, M. F.; Andrews, L. *J. Phys. Chem. A* **1998**, *102*, 8251.

(24) An experiment was done with Th and O_2 in neon: ThO was observed at 887.1 cm^{-1} and ThO_2 at 808.3 and 756.7 cm^{-1}. Gablenick, S. D.; Reedy, G. T.; Chasanov, M. G. *J. Chem. Phys.* **1974**, *60*, 1167 and references therein.

(25) Andrews, L.; Zhou, M. F. *J. Chem. Phys.* **1999**, *111*, 11044.

(26) Burkholder, T. R.; Andrews, L. *J. Chem. Phys.* **1991**, *95*, 8697.

(27) Hassanzadeh, P.; Andrews, L. *J. Phys. Chem.* **1992**, *96*, 9177.

(28) Andrews, L.; Spiker, R. C., Jr. *J. Phys. Chem.* **1972**, *76*, 3208.

(29) Thompson, W. E.; Jacox, M. E. *J. Chem. Phys.* **1989**, *91*, 3826.

(30) Frisch, M. J.; Trucks, G. W.; Schlegel, H. B.; Scuseria, G. E.; Robb, M. A.; Cheeseman, J. R.; Zakrzewaki, J. R.; Montgomery, J. A.; Stratmann, R. E.; Burant, J. C.; Dapprich, S.; Millam, J. M.; Daniels, A. D.; Kudin, K. N.; Strain, M. C.; Farkas, O.; Tomasi, J.; Barone, V.; Cossi, M.; Cammi, R.; B. Mennucci, B.; Pomelli, C.; Adamo, C.; Clifford, S.; Ochterski, J.; Petersson, G. A.; Ayala, P. Y.; Cui, Q.; Morokuma, K.; Malick, D. K.; Rabuck, A. D.; Raghavachari, K.; Foresman, J. B.; Cioslowski, J.; Ortiz, J. V.; Stefanov, B. B.; Liu, G.; Liashenko, A.; Piskorz, P.; Komaromi, I.; Gomperts, R.; Martin, R. L.; Fox, D. J.; Keith, T.; Al-Laham, M. A.; Peng, C. Y.; Nanayakkara, A.; Gonzalez, C.; Challacombe, M.; Gill, B. G. Hohnson, P. M. W.; Chen, W.; Wong, M. W.; Andrew, J. L.; Head-Gordon, M.; Replogle, E. S.; Pople, J. A. *Gaussian 98*, Revision A.1; Gaussian, Inc.: Pittsburgh, PA, 1998.

(31) Ismail, N.; Heully, J.-L.; Saue, T.; Daudey, J.-P.; Marsden, C. J. *Chem. Phys. Letts.* **1999**, *300*, 296.

(32) Becke, A. D. *Phys. Rev. A* **1988**, *38* 3098.

(33) Lee, C.; Yang, E.; Parr, R. G. *Phys. Rev. B.* **1988**, *37*, 785.

(34) Küchle, W.; Dolg, M.; Stoll, H.; Preuss, H. *J. Chem. Phys.* **1994**, *100*, 7535.

(35) Bouteiller, Y.; Mijoule, C.; Nizam, M.; Barthelat, J. C.; Daudey, J. P.; Pelissier, M.; Silvi, B. *Mol. Phys.* **1988**, *65*, 295.

(36) Maron, L.; Leininger, T.; Schimmelpfennig, B.; Vallet, V.; Heully, J.-L.; Teicteil, C.; Gropen, O.; Wahlgren, U. *Chem. Phys.* **1999**, *244*, 195.

(37) Pyykkö, P.; Li, J.; Runeberg, N. J. *J. Phys. Chem.* **1994**, *98*, 4809.

(38) van Wezenbeek, E. M.; Baerends, E. J.; Snijders, J. G. *Theor. Chim. Acta* **1991**, *81*, 139.

(39) Allen, G. C.; Baerends, E. J.; Vernooijs, P.; Dyke, J. M.; Ellis, A. M.; Fehrer, M.; Morris, A. *J. Chem. Phys.* **1988**, *89*, 5363.

(40) Following our suggestion, L. Maron and, V. Vallet (personal communication), have found a $^3\Phi_u$ ground state for UO_2 using AQCC methods and CASSCF orbitals.

(41) Gabelnick, S. D.; Reedy, G. T.; Chasanov, M. G. *J. Chem. Phys.* **1973**, *59*, 6397.

(42) Chertihin, G. V.; Andrews, L. *J. Phys. Chem.* **1995**, *99*, 6356. TiO_2 also increased 40% on annealing solid neon from 4 to 6 K.

(43) Howard, J. A.; Preston, K. F.; Mile, B. *J. Am. Chem. Soc.* **1981**, *103*, 6226.

(44) Kernisant, K.; Thompson, G. A.; Lindsay, D. M. *J. Chem. Phys.* **1985**, *82*, 4739.

(45) Citra, A.; Andrews, L. *J. Phys. Chem. A* **1999**, *103*, 4182.

(46) Kaledin, L. A.; Heaven, M. C. *J. Mol. Spectrosc.* **1997**, *185*, 1.

(47) Huber, K. P.; Herzberg, G. *Constants of Diatomic Molecules*; Van Nostrand Reinhold: New York, 1979.

(48) Heinemann, C.; Schwarz, H. *Chem. Eur. J.* **1995**, *1*, 7.

(49) Olander, D. R.; Yagnik, S. K.; Tsai, C. H. *J. Appl. Phys.* **1988**, *64*, 2680.